concentrations, is the absence of a reaction for regenerating water which could play a role comparable to that of reaction 5a in fairly dry tetraethylammonium bromide solution. The equilibrium

$$HO^- \text{ (or } DO^-) + H\text{-}CO\text{-}NMe_2 \rightleftarrows HO\text{-}H \text{ (or } DO\text{-}H) + [:CO\text{-}NMe_2]^- \quad (8)$$

certainly lies far to the left and hydroxide ion, formed when water transfers a hydrogen ion to a phenyl carbanion, cannot be readily converted back to water, as is the case when tetraethylammonium ion is present.

In runs 9 and 10 the nondeuterated benzene must have obtained almost all its protons directly from dimethylformamide (reaction 7), since deuterium would have been introduced by an indirect transfer (reaction 5 followed by reaction 8). The unfavorable equilibrium in reaction 8 also argues against the possibility of an indirect transfer. Further work is needed to establish which protons, "carbonyl" or "amide", are the reactive ones.

Another possible mode of reaction for the phenyl carbanion is addition to the carbonyl group of dimethylformamide (eq 9). We have detected small amounts of dimethylamine and

$$R:^- + H\text{—}CO\text{—}NMe_2 \longrightarrow R\text{—}\underset{\displaystyle H}{\overset{\displaystyle O^-}{\overset{|}{\underset{|}{C}}}}\text{—}NMe_2 \quad (9)$$

benzaldehyde in exploratory experiments but as yet have not had the opportunity to look systematically for byproducts which might result from such an addition.

After this work had been completed, Peters et al.[10] reported finding 0.002–0.05 mol % *N*-methylformamide (0.2–7 mM) in commercial grades of *N,N*-dimethylformamide. There is no question that the amide hydrogen of methylformamide is much more acidic than the carbonyl hydrogen of either methylformamide or dimethylformamide and would therefore donate protons more rapidly. However, we are currently using the same brands and grades of dimethylformamide as were used in the work reported here and find the monomethylformamide concentration to be consistently below 0.1 mM, our limit of detection.[11] This concentration is so much smaller than the amount of iodobenzene taken for reduction—40 mM in most experiments—that, even if all of the amide hydrogen had been consumed, dimethylformamide would still have to be the primary source of hydrogen.

Acknowledgments. The preliminary experiments which established the feasibility of this mass spectrometric approach were carried out by Mr. Kenneth W. Christrup as an undergraduate summer research project supported by the Uniroyal Foundation. The work reported here is taken in part from the M.A. Thesis of Ramon Alvarado de la Torre (Wesleyan University, 1974), whose graduate studies were supported by The American Scholarship Program of American Universities (LASPAU). We are indebted to Mr. Donald Albert for help with mass spectra and to Professors Albert Fry and Paul Haake for very helpful discussions.

References and Notes

(1) J. L. Webb, C. K. Mann, and H. M. Walborsky, *J. Am. Chem. Soc.*, **92**, 2042 (1970).
(2) J. R. Cockrell and R. W. Murray, *J. Electrochem. Soc.*, **119**, 849 (1972).
(3) M. F. Semmelhack, R. J. DeFranco, and J. Stock, *Tetrahedron Lett.*, 1371 (1972); M. F. Semmelhack and R. J. DeFranco, *J. Am. Chem. Soc.*, **94**, 8838 (1972).
(4) J. Grimshaw and J. Trocha-Grimshaw, *J. Chem. Soc., Perkin Trans. 2*, 215 (1975).
(5) R. C. Reed, Ph.D. Thesis, Wesleyan University, Middletown, Conn., 1970.
(6) R. S. Kittila, "Dimethylformamide Chemical Uses", E. I. du Pont de Nemours and Co., Wilmington, Del., 1967.
(7) Where it is necessary to distinguish between the isotopes of hydrogen, the appropriate symbol or word is used—"H", "D", "proton", "deuteron", etc. The terms "water", "hydrogen", and "hydroxide ion" are used in a general sense to include both isotopes.
(8) W. L. Underkofler and I. Shain, *Anal. Chem.*, **35**, 1778 (1963).
(9) L. W. Marple, *Anal. Chem.*, **39**, 844 (1967).
(10) G. M. McNamee, B. C. Willett, D. M. LaPerriere, and D. G. Peters, *J. Am. Chem. Soc.*, **99**, 1831 (1977).
(11) David E. Malerba, private communication.

Electrochemical Behavior of Tetrathiafulvalene-Tetracyanoquinodimethane Electrodes in Aqueous Media

Calvin D. Jaeger and Allen J. Bard*

Contribution from the Department of Chemistry, The University of Texas, Austin, Texas 78712. *Received August 3, 1978*

Abstract: Compacted pellets of tetrathiafulvalene-tetracyanoquinodimethane (TTF-TCNQ) were prepared and the properties of this material as an electrode in aqueous media were investigated. The electrode was stable over a potential range of about 0.9 V; within this region the electrode exhibited residual faradaic currents of less than 1–2 $\mu A/cm^2$ and the oxidation and reduction of soluble redox couples at this electrode could be carried out. Upon exceeding the potential limits of stability of the electrode, the subsequent voltammograms showed symmetrical peaks attributable to insoluble compounds of TTF or TCNQ and supporting electrolyte ions (e.g., TTFBr, KTCNQ). The redox reaction of these species could also be observed in the cyclic voltammograms.

Introduction

TTF-TCNQ and other organic metal-like compounds[1,2] have been the subject of extensive investigation by many groups.[3-7] For TTF-TCNQ most of the studies have concerned electrical and magnetic properties, crystal binding energies, and degree of charge transfer in the material. While there have been a few electrochemical studies of TTF and TCNQ compounds,[8-12] no studies have been reported concerning the utilization of TTF-TCNQ or other metal-like organic compounds as electrode materials. Only recently have the electrode properties of polymeric sulfur nitride, $(SN)_x$, been described.[13] While the properties and design of these organic metal-like

0002-7863/79/1501-1690$01.00/0

compounds have been investigated extensively, applications of these materials taking advantage of their unique electrical properties have not yet been developed. We report here an investigation of the electrochemical properties of TTF-TCNQ in aqueous solutions with a number of supporting electrolytes. These studies were designed to test the applicability of TTF-TCNQ (and other organic metal-like compounds) as electrodes for electrochemical studies and to obtain data on the redox properties of this material which might provide additional insight into its chemical behavior. Finally investigations of the electrochemistry of organic compounds such as TTF-TCNQ might provide information about organic semiconductor electrodes, which are of interest in photoelectrochemical studies.

Experimental Section

Electrode Preparation. The TTF-TCNQ complex was formed by mixing equimolar (~0.1 M) hot anhydrous acetonitrile solutions of neutral TCNQ and TTF. The black complex immediately precipitated as a microcrystalline powder. These crystals were washed with cold acetonitrile, then diethyl ether, and finally dried under vacuum. Larger single crystals could be formed by allowing acetonitrile solutions of the neutral species to diffuse together over a period of several weeks at a temperature of about 30 °C. The starting materials, TTF and TCNQ, were purified by several recrystallizations from benzene and by vacuum sublimation; TCNQ shows some decomposition during the sublimation, however. The dried TTF-TCNQ powder was fabricated into flat disks 0.5-1.0 mm thick, by pressing the microcrystalline powder in a 10-mm diameter die at a pressure of 2500-3000 psi. The disks thus formed had a black mirror-like appearance. The resistance of the electrode determined by forming a contact on both sides of the disk as described below was generally 1-5 Ω. Contacts were made to the disks by connecting a copper wire to one side with conducting silver epoxy (Allied Products Corp., New Haven, Conn.). An ohmic contact was confirmed by making a second contact to the other side of selected disks. In all cases the contact resistance was small and the current was directly proportional to the applied voltage. The back and sides of the electrode and the attached wire were sealed with nonconducting 5-min epoxy cement (Devcon Corp., Danvers, Mass.). The disks were then mounted on a glass tube and sealed to the glass with silicone adhesive (Dow Corning, Midland, Mich.). The electrode areas were typically 0.1-0.2 cm^2. Normally the electrodes were stored in a darkened vacuum desiccator until use. However, it was found that electrodes exposed to the atmosphere, even for several months, showed similar behavior or in a few cases were only slightly oxidized. Air-oxidized electrodes showed a small cathodic peak in the initial cyclic voltammogram within the stable potential region.

Chemicals. The TTF was synthesized by the procedure of Melby.[14] Other TTF samples were purchased from Aldrich Chemical Co. (Milwaukee, Wis.), as was the TCNQ. The acetonitrile was spectroscopic grade quality which had been distilled several times from P_2O_5. All other chemicals were reagent grade.

Electrochemical Apparatus. The electrochemical cell consisted of a single-compartment cell with two side arms opposite each other. The counter electrode was a platinum wire inside a glass tube separated from the main compartment by a glass frit. The reference electrode was a saturated calomel electrode (SCE). The auxiliary and reference electrodes were inserted into the cell side arms. One side of the cell had an optically flat Pyrex window. As many as three different working electrodes could be inserted through the top at the same time. Before each experiment the solution was deaerated with purified nitrogen. During the experiments either the N_2 flow was stopped and the cell sealed or the flow of N_2 was continued above the solution. A PAR Model 173 potentiostat and PAR Model 175 universal programmer (Princeton Applied Research Corp., Princeton, N.J.) were used for the electrochemical experiments. The data was recorded on a Houston Instruments (Austin, Texas) Model 2000 *XY* recorder. The capacitance was measured with a Wenking 61 RH potentiostat (G. Bank Electonik, West Germany) and PAR Model 5204 lock-in analyzer, from the magnitude and phase angle of the current at different frequencies. The electron micrographs were taken with a scanning microscope (SEM) JSM-2 (Japan Electron Optical Laboratory Co., Ltd.). A 450-W xenon lamp and power supply (Oriel Corp., Stamford, Conn.) was used as the light source. Resistance compensation was used in all experiments by adjusting the amount of positive feedback just short of potentiostatic oscillation as monitored by an oscilloscope.

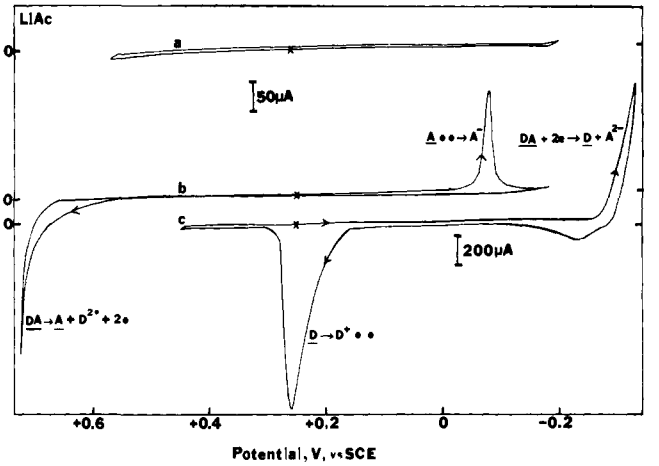

Figure 1. Cyclic voltammogram of the TTF-TCNQ electrode in 1 M lithium acetate at a scan rate of 5 mV/s: (a) stable potential region; (b) oxidation of the electrode surface and resultant peak on reversal; (c) reduction of the electrode surface and the resultant peak on reversal. In all figures A and D represent TCNQ and TTF, respectively. Insoluble or slightly soluble species are underlined. Scans start at potential marked by X.

Results

The TTF-TCNQ electrode disks were very stable at open circuit in aqueous media. Even electrodes immersed in distilled water for several weeks appeared relatively unchanged and still gave a potential region with no observed current peaks attributable to decomposition products. The available potential limits of stability of the TTF-TCNQ electrode appear to be influenced only very slightly by the nature of the supporting electrolyte, although small variations were found when the electrolyte contained ions which formed an insoluble compound with either $TCNQ^-$ or TTF^+ (e.g., K^+, Cl^-, Br^-). Generally a potential region of electrode stability from +0.5 to −0.2 V vs. SCE was found with any supporting electrolyte (Figure 1a). Within this stable potential region selected redox couples, such as $Fe(CN)_6^{3-}/Fe(CN)_6^{4-}$ or Cu(II)/Cu(I)(1 M KCl), could be oxidized or reduced (Figure 2). For both couples the resultant cyclic voltammograms at a TTF-TCNQ electrode and a Pt disk electrode showed peaks at about the same potentials. The observed differences in peak currents in Figure 2 are due to different electrode areas. The peak separations (ΔE_p) at the TTF-TCNQ electrode for the $Fe(CN)_6^{3-}/Fe(CN)_6^{4-}$ and Cu(II)/Cu(I) couples were 62 ± 3 and 57 ± 3 mV, respectively. Even after more than 20 cycles with these couples, the surface of the TTF-TCNQ electrode remained unchanged. When the TTF-TCNQ electrode was placed in 1 M NaOH and a positive potential sufficient to cause oxidation of the electrolyte was applied, the electrode surface did become pitted after prolonged oxidation. Iodine could be generated at the TTF-TCNQ electrode by oxidation of a 0.1 M KI solution; the electrogenerated I_3^- showed no apparent reaction with the electrode. In addition, metals such as copper could be electrodeposited and then anodically stripped from a TTF-TCNQ electrode (from a 20 mM $CuSO_4$, 1 M potassium acetate solution) without affecting the nature of the electrode surface. Thus in the region of electrode stability, reversible electrochemical behavior of several redox couples is observed, demonstrating the metallic behavior of the TTF-TCNQ electrode.

Electrode Decomposition Reactions and Products. If the potential is scanned beyond the stable region in either the negative or positive direction, a charge transfer reaction occurs

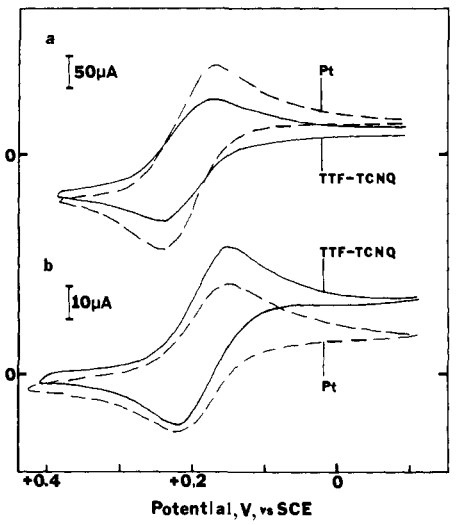

Figure 2. Comparison of Pt and TTF-TCNQ electrodes for cyclic voltammetry of soluble solution species: (a) 15 mM $K_3Fe(CN)_6/K_4Fe(CN)_6$ in acetic acid/potassium acetate (pH 6.9); (b) 10 mM $CuCl_2$ in 1 M KCl. Scan rate, 5 mV/s. —, TTF-TCNQ electrode; - - - - -, Pt disk electrode.

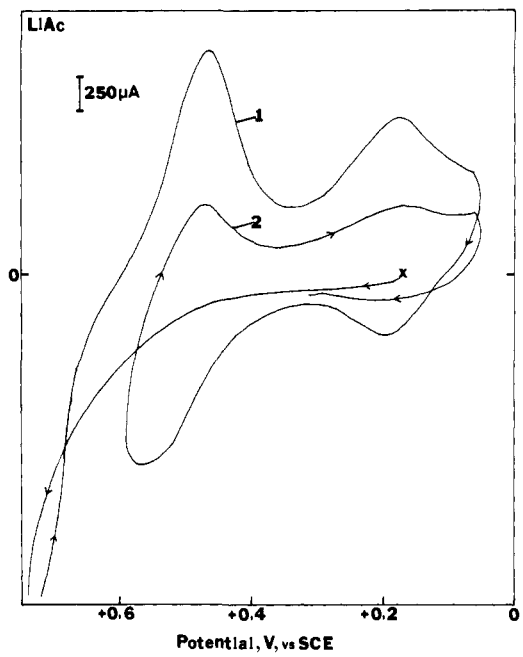

Figure 3. Cyclic voltammogram of TTF-TCNQ electrode in 1 M lithium acetate at scan rate of 500 mV/s. (1) The first scan after oxidation of the electrode surface; (2) second scan.

Table I. Coulometric Measurements for the Reduction and Oxidation of the TTF-TCNQ Electrode[a]

electrolyte	initial process	charge[b] passed, mC	reversal process	charge[b] passed, mC
1 M LiAc	oxidn, +0.65 V	3.95	redn, −0.04 V	−2.02
	redn, −0.27 V	−56.3	oxidn, +0.15 V	28.5
1 M LiCl	oxidn, +0.50 V	3.95	redn, −0.04 V	−2.02
	redn, −0.28 V	−7.34	oxidn, +0.13 V	5.42
1 M KBr	oxidn, +0.49 V	13.8	redn, +0.03 V	−7.87
			oxidn,[c] +0.26 V	7.55

[a] Each pair of measurements was made with different electrodes of slightly different areas (0.1 cm^2) and involves different extents of oxidation and reduction. All potentials are in V vs. SCE. [b] Calculated for 1 cm^2 TTF-TCNQ monolayer, 0.014-0.043 mC.[15] [c] Second reversal.

caused by reduction or oxidation of the electrode itself. The behavior depends on the nature of the supporting electrolyte and the solubilities of the salts formed by TTF and TCNQ ions with supporting electrolyte ions. The behavior of the TTF-TCNQ electrode in aqueous solutions of supporting electrolyte M^+X^- illustrates the four possible cases: (1) M^+TCNQ^- and TTF^+X^- are both soluble, lithium acetate; (2) M^+TCNQ^- is soluble and TTF^+X^- is only partially soluble, lithium chloride; (3) M^+TCNQ^- is insoluble and TTF^+X^- is soluble, potassium acetate; (4) both M^+TCNQ^- and TTF^+X^- are insoluble, potassium bromide.

Lithium Acetate. The behavior of the TTF-TCNQ electrode in 1 M LiAc is shown in Figure 1. The Li^+TCNQ^- salt is soluble in water. Although the acetate salt of TTF^+ has not been described previously, we found that it is also water soluble. When the applied potential is brought outside the stable region (i.e., to beyond about +0.65 V), an anodic current was observed that clearly resulted from oxidation of the electrode. The once shiny black electrode surface turned yellow and a yellowish color was seen in solution near the electrode surface. This oxidation corresponds to the formation of $TCNQ^0$ and TTF^{2+} at the electrode surface.

$$TTF\text{-}TCNQ(s) - 2e^- \rightarrow TTF^{2+}(aq) + TCNQ^0(s) \quad (1)$$

Justification of this and all other observed reactions will be given later. If the scan continues in a positive direction the resultant current continues to increase (scan b), much like the dissolution of a metal electrode. This is expected if, as the electrode is oxidized, one of the resulting products is soluble in solution and dissolves from the surface of the electrode providing more unreacted surface to be oxidized. Eventually the entire surface turned yellow and, after sufficient extent of electrolysis, the current dropped to zero. At this point the yellow surface behaved as an insulating layer and the potential limits of the electrolyte could be exceeded without any observable current. When the scan was reversed to a negative direction, no faradaic current was observed until −0.04 V, where a cathodic peak occurred. The yellow surface of the electrode disappeared during this reduction and a bluish substance left the electrode surface and moved into the bulk of the solution. This corresponds to the reduction of $TCNQ^0$ to a soluble species:

$$TCNQ^0(s) + e^- \rightarrow TCNQ^-(aq) \quad (2)$$

If the scan direction was reversed toward positive potentials following this cathodic peak, no other peaks were observed between −0.04 V and the positive limit. If this anodic scan was reversed before the positive (anodic) limit was again attained, the cathodic peak at −0.04 V was no longer found. The electrode surface now appeared black, but was no longer shiny. Coulometric measurements show that the integrated area of the cathodic peak at −0.04 V is one-half the number of coulombs passed in the oxidation of the lattice (Table I), as predicted from eq 1 and 2. The voltammograms shown in Figure 1 were obtained at a scan rate of 5 mV/s. During this very slow scan, any species formed which were soluble in solution left the electrode surface because of natural convection and were not detected on a reverse scan. If a scan rate of 0.5 V/s was used, when the positive limit of a TTF-TCNQ electrode was exceeded and the scan immediately reversed, two sets of peaks occurred between the positive limit of the electrode and +0.4 V (Figure 3). These peaks are ascribed to the TTF^{2+}/TTF^+ and TTF^+/TTF^0 couples. Scan reversals between +0.6 (short of further electrode oxidation) and +0.4 V continued to show the waves, which greatly diminished in magnitude because of diffusion of solution species away from the electrode surface. If, upon reducing the yellow oxidized surface, the scan direc-

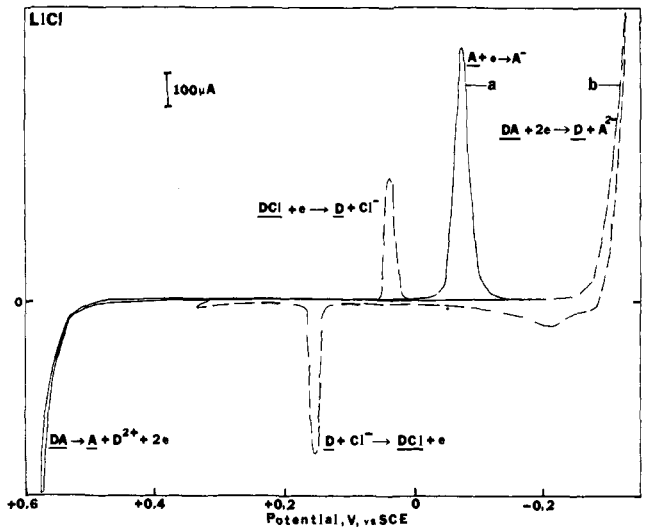

Figure 4. Cyclic voltammogram of the TTF-TCNQ electrode in 1 M lithium chloride: (a) solid line, positive scan with oxidation of the electrode surface and reversal; (b) dashed line, negative scan with reduction of the electrode surface and reversal. Scan rate, 5 mV/s.

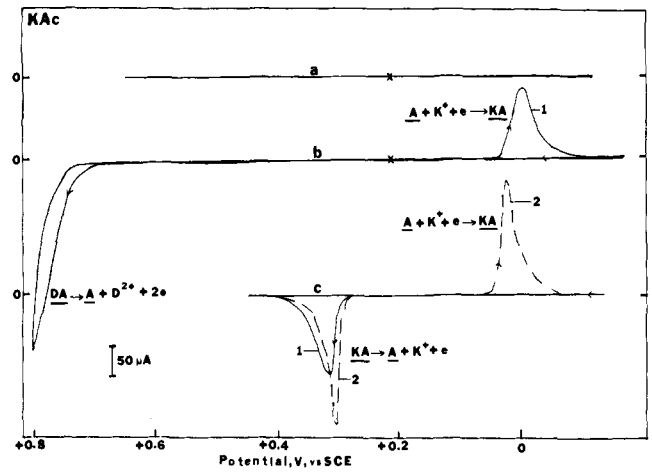

Figure 5. Cyclic voltammograms of the TTF-TCNQ electrode in 1 M potassium acetate, result of lattice oxidation: (a) potential region where the electrode showed little faradaic current due to electrode decomposition; (b) positive scan with oxidation of the electrode surface and reduction peak on reversal; (c) observed peaks following lattice oxidation for repetitive scans between −0.1 and +0.4 V; (1) —, first scan; (2) - - -, second and succeeding scans. Scan rate, 5 mV/s.

tion was reversed to a positive direction at a scan rate of 0.5 V/s, an anodic peak was observed at +0.18 V.

If the negative limit of the electrode (about −0.28 V) was exceeded, a large dissolution current, again similar to that observed for metal dissolution, occurred (Figure 1c). This reduction resulted in the formation of TTF^0 and $TCNQ^{2-}$ being formed at the electrode surface.

$$TTF\text{-}TCNQ(s) + 2e^- \rightarrow TTF^0(s) + TCNQ^{2-} \quad (3)$$

The electrode surface became light colored with some blue appearing in the solution near the electrode during the reduction. Upon reversing the scan direction a small anodic current peak at −0.2 V was observed. The blue color in solution intensified during the oxidation. At a potential of ~+0.20 V an anodic peak occurred and the electrode surface changed to a dark color with a dark brown substance observed going into solution. This represents the oxidation of the TTF^0 formed in the background reduction:

$$TTF^0(s) - e^- \rightarrow TTF^+(aq) \quad (4)$$

Coulometric measurements showed that the area of this anodic wave involved one-half of the amount of electricity passed during the cathodic reaction at −0.28 V (Table I). Subsequent scans between +0.60 and −0.20 V showed no peaks.

Lithium Chloride. The use of a chloride-containing electrolyte differs from an acetate electrolyte, since TTF^+Cl^- is only slightly soluble in water. The oxidation of the lattice in 1 M LiCl proceeded in an analogous manner as for LiAc, eq 1, except that the oxidation started at +0.50 V (Figure 4). Upon reversing the scan, no faradaic current was observed until −0.04 V, where the yellow $TCNQ^0$ surface was reduced. Again the yellow surface disappeared and the blue $TCNQ^-$ was seen diffusing from the surface, eq 2. Coulometric measurements again showed a 2:1 ratio between the oxidation of the lattice and the observed cathodic peak at −0.04 V (Table I).

If the negative limit of the electrode was exceeded (Figure 4), the lattice was reduced at −0.28 V, eq 3. The wave continued to increase and exhibited the same behavior as for LiAc. However, when the scan was reversed toward a positive direction, a new anodic peak at +0.13 V occurred. This corresponds to the formation of $TTF^+Cl^-(s)$.

$$TTF^0(s) + e^- + Cl^-(aq) \rightarrow TTF^+Cl^-(s) \quad (5)$$

The surface of the electrode turned from a light color to a purple. If the scan direction was now reversed, a cathodic peak was observed at +0.05 V, representing reduction of the $TTF^+Cl^-(s)$, in the reverse of eq 5. The color of the electrode changed from a deep purple to a lighter color during this reduction step. Subsequent scans between 0.0 and +0.2 V continued to show these two peaks with essentially no change in magnitude, although they gradually decreased in size over a time period of 10–20 min, probably because one of the species dissolved slightly. If, after the anodic peak at +0.13 V, the scan was continued in a positive direction, the electrode remained unchanged until about +0.39 V, where a wave occurred and a brown substance was observed diffusing from the electrode. This probably represents the oxidation of $TTF^+Cl^-(s)$.

$$TTF^+Cl^-(s) - e^- \rightarrow TTF^{2+} + Cl^- \quad (6)$$

Upon reversing the scan direction the cathodic peak previously observed at +0.05 V had almost disappeared. If more scans were made between the potential limits (+0.5 and −0.20 V), eventually no peaks were observed and the electrode was again black.

Potassium Acetate. The initial and subsequent voltammograms for a TTF-TCNQ electrode in a 1 M potassium acetate solution are shown in Figure 5. The solubility of the K^+TCNQ^- salt in water is very small (10^{-11} mol/L).[10] The oxidation of the electrode started at about +0.65 V, as observed with the LiAc electrolyte. If the potential scan was reversed, no faradaic current was observed until +0.04 V. At this potential a cathodic peak occurred and the yellow surface of the electrode turned reddish purple (scan b). In this case the reduction of $TCNQ^0(s)$ results in the formation of the insoluble $K^+TCNQ^-(s)$.

$$TCNQ^0(s) + K^+(aq) + e^- \rightarrow K^+TCNQ^-(s) \quad (7)$$

If the scan direction was reversed toward positive potentials, an oxidation peak occurred at +0.29 V, representing the oxidation of the $K^+TCNQ^-(s)$, in the reverse of eq 7 (scan c). The areas of the two peaks at +0.04 and +0.29 V were nearly equal. The surface of the electrode after reoxidation again appeared yellow, with no material noticed going into solution. If, as in the case of LiAc, the lattice was oxidized and the scan immediately reversed at 0.5 V/s, then two sets of peaks, as in Figure 3, which gradually disappear on scanning only over these peaks, were observed. The areas of the two peaks at +0.04 and +0.29 V remained relatively constant upon cycling between +0.50

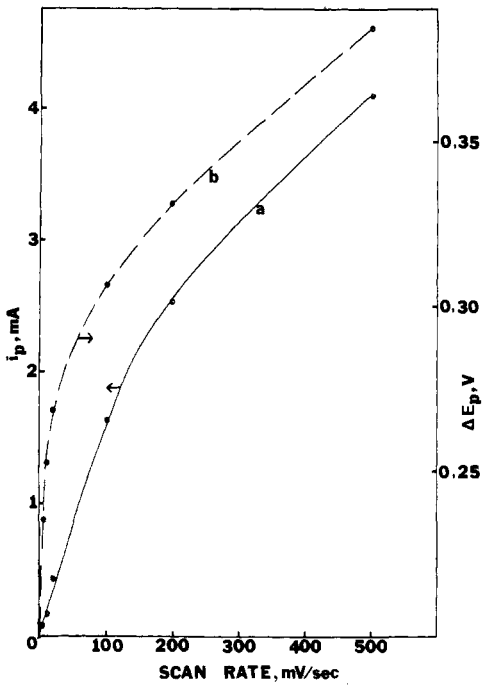

Figure 6. Scan rate dependence of cyclic voltammetric (a) peak heights (i_p) and (b) peak potential separations (ΔE_p) for the TCNQ/TCNQ$^-$K$^+$ waves (Figure 5c) on a TTF-TCNQ electrode prepared by lattice oxidation in 1 M KAc followed by cycling between +0.4 and −0.15 V vs. SCE at 5 mV/s until peak heights were constant. i_p represents average of i_{pc} and i_{pa}.

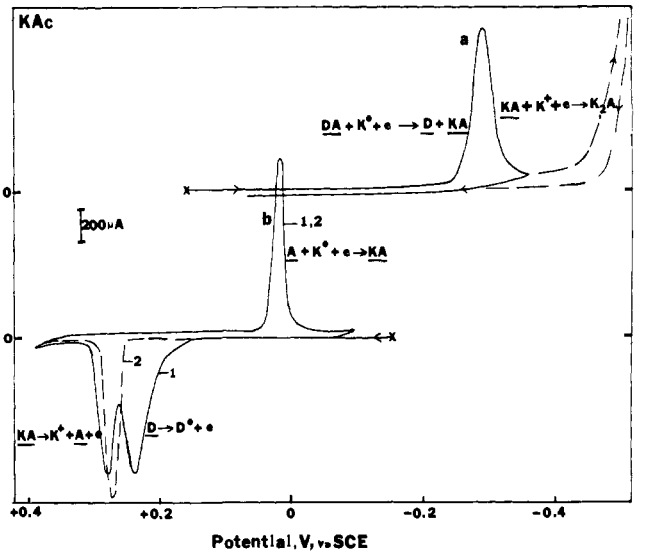

Figure 7. Cyclic voltammogram of the TTF-TCNQ electrode in 1 M potassium acetate; result of lattice reduction: (a) negative scans with reduction of the electrode surface; (b) observed peaks on reversal following reduction of the surface; (1) first scan; (2) second scan. Scan rate, 5 mV/s.

and −0.10 V. After over 80 cycles taken over a period of about 1 h, the magnitude of the peaks had decreased by less than 6%. Cyclic voltammetric experiments demonstrate that these two peaks are directly linked. If, for example, during the cycling, the scan was reversed just positive of the cathodic peak, no anodic peak was found. Similarly no cathodic peak was found if the anodic peak was not traversed first. We conclude that the same couple is responsible for both peaks showing a peak separation of ~0.25 V.

If the potential limits were set so as to just include the peaks occurring at +0.04 and +0.29 V, these peaks, as indicated earlier, remained over repeated scans with only a slight decrease in magnitude. The dependence of the peak currents (i_p) of these peaks with scan rate (v) was investigated; typical results are shown in Figure 6. For scan rates up to 100 mV/s i_p values for both anodic (i_{pa}) and cathodic (i_{pc}) peaks were directly proportional to v, as expected for the reversible reduction and oxidation of surface species. Above this value the i_p values fell off, suggesting the onset of mass transfer or kinetic limitations.

The cyclic voltammograms resulting from exceeding the negative limits of the electrode are shown in Figure 7. At a potential of −0.30 V a cathodic peak was observed (scan a), attributed to reduction of the electrode surface. As the peak was traversed the color of the surface changed from a black to a light reddish-purple. As indicated previously this is believed to correspond to the formation of TTF^0(s) and K^+TCNQ^-(s):

$$TTF\text{-}TCNQ(s) + K^+(aq) + e^- \rightarrow TTF^0(s) + K^+TCNQ^-(s) \quad (8)$$

If the scan was reversed, two anodic peaks were observed (scan b). At +0.26 V dark brown material came off the electrode surface. If the scan was continued in a positive direction, the second anodic peak at +0.29 V was observed and the electrode surface turned yellow. The first oxidation corresponds to the oxidation of TTF^0(s) (eq 4) and the second to the oxidation of K^+TCNQ^-(s) (reverse of eq 7). Note that the second peak occurred at the same place as that found after oxidation and scan reversal as described above. Upon reversing the scan a single cathodic peak corresponding to reduction of the deposited $TCNQ^0$(s) (eq 7) was observed (scan b) and the surface of the electrode became now reddish-purple. Reversing the scan immediately following this peak resulted in only the anodic peak at +0.29 V, since the TTF^+ formed during the first anodic scan had left the electrode surface at this slow scan rate. Just as in the case of the peaks resulting from exceeding the positive limit, the two peaks at +0.29 and +0.04 V were nearly equal in magnitude and were clearly linked. Unlike the insulating behavior noted when the positive limit was exceeded, when the negative scan was continued beyond the peak at −0.30 V, another reduction occurred at −0.56 V (scan a). The current here increased without limit; the process here probably represents the reduction of K^+TCNQ^-(s):

$$K^+TCNQ^-(s) + e^- \rightarrow TCNQ^{2-} + K^+ \quad (9)$$

No anodic peak corresponding to oxidation of the reduction product was found on scan reversal.

Potassium Bromide. The most complex behavior was observed with a 1 M KBr solution, since both K^+TCNQ^- and TTF^+Br^- are insoluble. However, the behavior can be interpreted by comparison of the cyclic voltammograms to those obtained with the other electrolytes. Oxidation of the lattice occurred at +0.49 V (Figure 8b). The electrode turned yellow and some brown material left the surface. The oxidation reaction is given by

$$TTF\text{-}TCNQ(s) + 2Br^- + 2e^- \rightarrow TCNQ^0(s) + TTF^{2+}(Br^-)_2(s) \quad (10)$$

If the scan direction was reversed, a small peak was observed at +0.44 V, which probably corresponds to the reduction of $TTF^{2+}(Br^-)_2$ formed during the oxidation of the lattice.

$$TTF^{2+}(Br^-)_2(s) + e^- \rightarrow TTF^+ + 2Br^- \quad (11)$$

The greater the extent of electrode oxidation, the larger was the cathodic peak at +0.44 V. Another very broad cathodic peak was observed at +0.18 V. It appears that this species is in solution and not a solid at the electrode surface. If the scan continued in a negative direction, the electrode surface was

reduced in a cathodic peak at +0.04 V and the yellow surface turned a reddish-purple color. This peak was the same as that observed with KAc and again corresponds to the formation of K^+TCNQ^- (reverse of eq 7). Upon reversing the scan, the electrode remained unchanged until +0.29 V (scan b), where an anodic peak corresponding to oxidation of $K^+TCNQ^-(s)$ (eq 7) occurred and the electrode color again became yellow. Coulometric measurements showed a 2:1 ratio between the number of coulombs passed in the oxidation of the lattice and those for the reduction peak at +0.04 V (Table I). The area of the peak at +0.04 V was equal to that of the anodic peak at +0.29 V. These two peaks continued to be observed for repetitive scans between the potential limits of +0.40 and −0.15 V.

Reduction of the lattice began at −0.26 V in an analogous manner as for KAc (scan a). The observed peak appears to be the superposition of two waves, one due to a surface process and another characteristic of some diffusion-controlled process. During this reduction the electrode surface changed from black to a light reddish-purple color. When the potential scan was reversed, two anodic peaks at +0.08 and +0.28 V occurred. The color changed to a dark purple during the first oxidation peak and to a light color during the second. If again the scan was reversed, two cathodic peaks appeared at +0.05 and −0.09 V. Again the color of the electrode changed, first to a deep purple and then to a lighter purple. Subsequent scans between +0.45 and −0.20 V continued to show these four peaks, the anodic ones at +0.29 and +0.08 V and the cathodic ones at +0.04 and −0.15 V. The pair of peaks +0.04 and +0.29 V are related and clearly belong to the $K^+TCNQ^-(s)/TCNQ^0(s)$ couple. The pair of peaks at −0.15 and +0.08 V can then be ascribed to the $TTF^+Br^-(s)/TTF^0(s)$ pair. Thus the TTF-TCNQ reduction peak reaction can be written

$$TTF\text{-}TCNQ(s) + K^+(aq) + e^- \rightleftarrows TTF^0(s) + K^+TCNQ^-(s) \quad (12)$$

and, on reversal, eq 7 and

$$TTF^0(s) + Br^-(aq) - e^- \rightleftarrows TTF^+Br^- \quad (13)$$

As with potassium acetate, if the applied potential was continued negative of the wave at −0.26 V an increasing cathodic current was observed at −0.5 V. No new anodic peaks following this limiting reduction were observed. Another feature of the resultant cyclic voltammograms was the observation of an anodic peak at +0.52 V and its corresponding cathodic peak at +0.44 V. These peaks are probably due to the formation of $TTF^{2+}(Br^-)_2$ and then the reduction of this species (eq 11).

$$TTF^+Br^- - e^- + Br^- \rightarrow TTF^{2+}(Br^-)_2 \quad (14)$$

Similar behavior was observed for SCN^- electrolyte. In Figure 8, scan c, the cyclic voltammogram of the TTF-TCNQ electrode including all resultant peaks is shown.

The relative areas of the voltammetric peaks and the coulometric measurements shown in Table I support the proposed reactions. In general (1) the number of coulombs consumed upon lattice oxidation is about twice that of the resultant cathodic peak found in scan reversal; (2) this cathodic peak area is about equal in magnitude to the corresponding anodic peak area upon a second reversal; (3) the area of the anodic peak found upon scan reversal is equal to or greater than one-half of the coulombs passed on reduction of the lattice. In all cases the coulometric measurements show that the amount of material being oxidized or reduced is much larger than one monolayer.[15] To make sure that the actual (electrochemical) area of the electrode was about the same as the geometric one, the chronoamperometric reduction of $Fe(CN)_6^{3-}$ at the TTF-TCNQ electrode was investigated. The solution contained

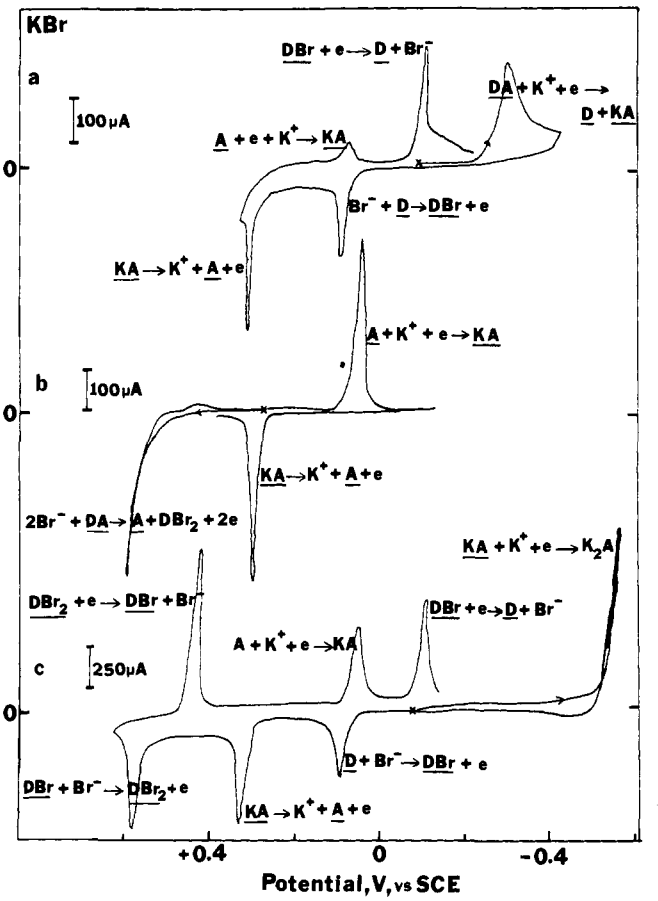

Figure 8. Cyclic voltammogram of the TTF-TCNQ electrode in 1 M potassium bromide: (a) initial negative scan with reduction of the electrode surface and resultant peaks on reversal; (b) initial positive scan with oxidation of the electrode surface and resultant peaks on reversal; (c) after the electrode surface has been oxidized and reduced. Scan rate, 5 mV/s.

5-20 mM $K_3Fe(CN)_6^{3-}$ in 1 M KCl and measurements of i were carried out for times (t) between 0.2 and 26 s. From the values of $it^{1/2}$ vs. C, assuming Cottrell behavior and a diffusion coefficient of $Fe(CN)_6^{3-}$ of $0.763 \pm 0.01 \times 10^{-5}$ cm^2/s,[16] the area was determined. In general, electrochemically measured areas were not significantly different than measured geometric areas. For example, a typical area determined in this way was 0.119 cm^2, compared with the geometrically measured area of 0.12 cm^2.

The relatively large amounts of material oxidized or reduced (of the order of hundreds of monolayers) suggests that as the electrolysis occurs the electrode becomes sufficiently porous and that solution can have access to the underlying layers; this is especially important when an insulating material such as $TCNQ^0$ is produced. The change in the electrode surface after oxidation is clearly seen in scanning electron microscope (SEM) photographs (Figure 9).

Other Supporting Electrolytes. The behavior of the TTF-TCNQ electrode was studied in a number of other supporting electrolytes (Table II). In supporting electrolyte containing Br^-, Cl^-, I^-, and SCN^-, the response of the TTF-TCNQ electrode indicated that insoluble compounds with TTF^+ were formed. For Ac^- and F^- supporting electrolytes, the TTF^+ was soluble. Similarly the behavior of the TTF-TCNQ electrode was different in the presence of different cations, with peaks ascribable to insoluble salts of $TCNQ^-$ found with all cations other than Li^+. In 1 M HAc the oxidation of the TTF-TCNQ electrode resulted in very broad peaks. Upon adding KAc the peaks became sharper and the peak potential shifted slightly.

Table II. Potentials for Lattice Oxidation and Reduction and Peaks on Reversal for TTF-TCNQ Electrodes in Various Supporting Electrolytes[e]

supporting electrolyte	lattice oxidn[a]	redn peaks on reversal	oxidn peaks on second reversal	lattice redn[a]	oxidn peaks on reversal	redn peaks on second reversal
1 M LiI[b]				−0.25	+0.02	−0.16
1 M LiBr	+0.49	+0.42		−0.22	+0.09	−0.06
		−0.05				
1 M LiF	+0.50	−0.13		−0.21	+0.27	
1 M LiCl	+0.50	−0.04		−0.28	+0.13	+0.05
1 M LiAc	+0.65	−0.08		−0.27	+0.32	
					(0.16[a])	
1 M KI[b]				−0.19[c]	+0.01	−0.19
1 M KBr	+0.49	+0.04	+0.26	−0.26[c]	+0.08	−0.09
					+0.28	+0.05
					+0.52[d]	+0.41[d]
1 M KCl	+0.54	+0.03	+0.25	−0.25[c]	+0.16	+0.03
1 M KAc	+0.65	+0.04	+0.29	−0.30[c]	+0.26	+0.03
					+0.29	
1 M KSCN				−0.29	−0.02	−0.19
					+0.27	+0.05
					+0.38	+0.15
1 M NaAc	+0.67	+0.01	+0.28	−0.29[c]	+0.24	+0.02
					+0.28	
1 M HAc	+0.52	+0.02	+0.43	−0.30[c]	+0.18	−0.11
		(0.12[a])	(0.15[a])			
					+0.39	0.0
1 M $PbAc_2$	+0.58	−0.01	+0.12	−0.23	−0.01	−0.26
				(−0.38[c])		
					+0.25	0.0
1 M $CaAc_2$	+0.63	−0.03	+0.12	−0.21	+0.19	−0.05
					+0.30	
1 M $BaAc_2$	+0.60	+0.01	+0.13			
1 M $CdAc_2$	+0.69	+0.01	+0.10			
1 M NH_4Cl	+0.51	+0.01	+0.18	−0.22	+0.14	+0.03
				(−0.32[c])		
					+0.22	−0.06
1 M NH_4SCN				−0.19	−0.01	−0.20
				(−0.23[c])		
					+0.19	0.0
1 M $NiCl_2$	+0.50	+0.02	+0.17			
1 M $CaCl_2$				−0.24	+0.12	−0.05
					+0.15	+0.05

[a] Potential of the onset of faradaic current; ([c]) indicates location of peak for this process, when observed. [b] Positive potential limit was +0.15. [c] Peak potential. [d] Peaks were most prominent after reduction of the lattice; when the oxidation of the lattice was continued until an insulating layer formed these peaks were observed upon subsequent reversal. [e] All potentials in V vs. SCE.

Eventually, upon adding more KAc, the behavior became similar to that in KAc supporting electrolyte.

Behavior of TTF^0/C and $TCNQ^0$/C Electrodes. To obtain information about the behavior of TTF and TCNQ alone, mixtures of TTF and carbon (graphite powder, grade 38, Fisher) and TCNQ and carbon (1:1 by weight) were prepared. Compressed disks of these mixtures, ca. 1 mm thick and 0.5 cm^2 area, were made into electrodes. In Figures 10 and 11, the behavior of these electrodes in 1 M LiAc and 1 M KSCN is shown. In general any observed peaks were larger and showed larger peak areas than those found with TTF-TCNQ electrodes. The potential for the onset of the anodic or cathodic current and for these peaks corresponded very closely to the behavior found for similar half-reactions with the TTF-TCNQ electrode. Compare, for example, the potentials for the D^+/D and A/A^- couples in LiAc (Figures 1 and 10) or the A/KA couples (Figures 5 and 11). Potentials for the oxidation and reduction processes at these electrodes are summarized in Table III.

Double Layer Capacitance Measurements. The background currents for the TTF-TCNQ electrode in the stable region appeared much larger than those for a platinum electrode of the same area. To determine if this could be ascribed to purely a capacitive charging current, measurements of the double layer capacitance, C_{dl}, of the TTF-TCNQ electrode-solution interface in this region were undertaken. C_{dl} was determined by two methods. The dc potential of the electrode was adjusted to a value in the stable region, e.g., +0.2 V. Superimposed on this applied potential was an ac signal of 5 mV. From the magnitude and phase angle of the resulting ac current as measured with a lock-in amplifier, the capacitance and resistance were determined. The second method consisted of scanning the potential in the stable region and measuring the current, i, as a function of scan rate, v. C_{dl} was then calculated from the equation $C_{dl} = i/v$. Typical apparent C_{dl} values determined by these methods are shown in Figure 12. Generally the C_{dl} was frequency dependent, decreasing with increasing scan rate or frequency, with the two methods showing reasonable agreement in overlapping frequency ranges. For example, one TTF-TCNQ electrode in 1 M KCl showed a C_{dl} = 490 $\mu F/cm^2$ at v = 2 mV/s and C_{dl} = 319 $\mu F/cm^2$ at v = 100 mV/s. Using the impedance method, a different electrode in 1 M KCl (at +0.190 V vs. SCE) showed C_{dl} = 186 $\mu F/cm^2$ at 100 Hz and C_{dl} = 27 $\mu F/cm^2$ at 10 kHz. If the TTF-TCNQ electrode is changing during these measurements, this may account for some of the discrepancies that have been observed.

Photoeffects. Although photoeffects were not expected with

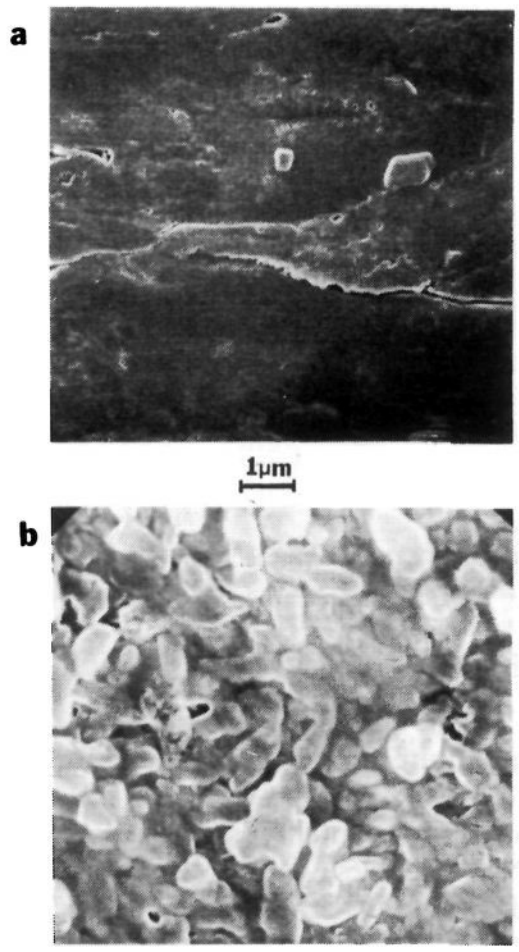

Figure 9. Scanning electron micrograph at 5000× magnification of (a) unreacted disk of TTF-TCNQ; (b) TTF-TCNQ electrode which was oxidized in 1 M KAc.

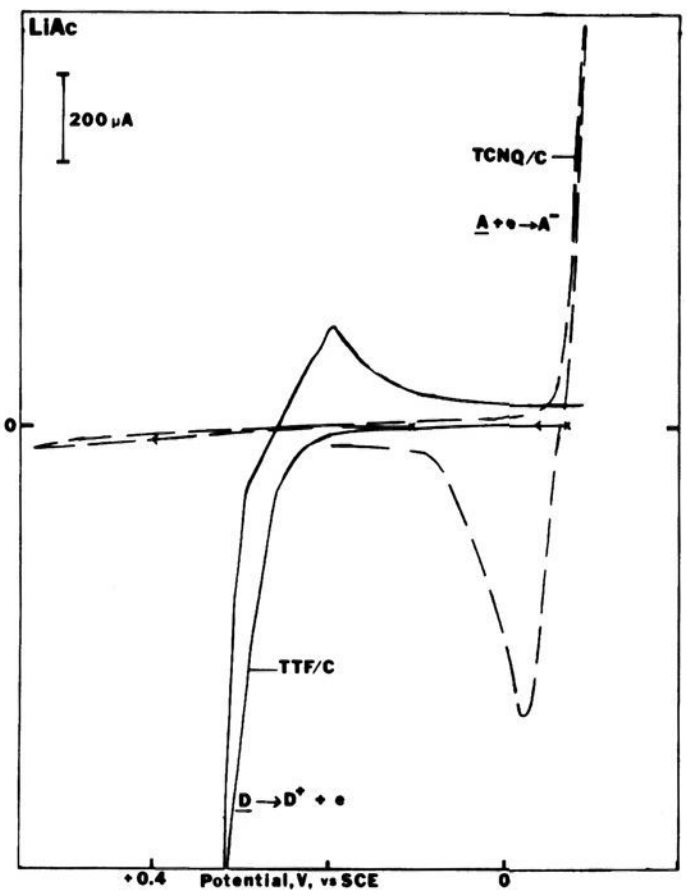

Figure 10. Cyclic voltammogram of a TTF/C and TCNQ/C electrode in 1 M LiAc at scan rate of 5 mV/s.

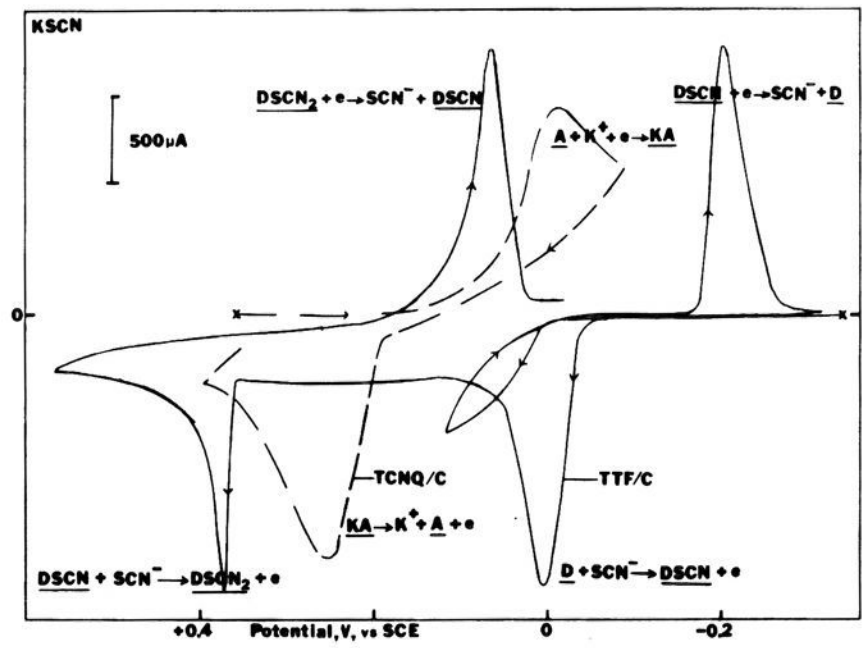

Figure 11. Cyclic voltammogram of a TTF/C and TCNQ/C electrode in 1 M KSCN at scan rate of 5 mV/s.

Table III. Potentials (V) for Oxidation and Reduction and Scan Reversal Processes for TTF/C, TCNQ/C, and MTCNQ/C Electrodes[a]

	TTF/C Electrode			
supporting electrolyte	initial scan oxidns[c]		redns on scan reversal[c]	
1 M KAc	+0.23		+0.25 (+0.20[b])	
1 M LiAc	+0.24		+0.26 (+0.19[b])	
1 M KCl	+0.14 (0.26[b])	+0.53[b]	+0.08 (+0.01[b])	+0.33[b]
1 M KBr	+0.06 (0.14[b])	+0.58[b]	−0.05 (−0.17[b])	+0.39[b]
1 M KSCN	−0.04	+0.38[b]	−0.19 (−0.27[b])	+0.08[b]

	TCNQ/C Electrode	
supporting electrolyte	initial scan redns[c]	oxidns on scan reversal[c]
1 M KAc	+0.05 (−0.05[b])	+0.19 (+0.30[b])
1 M KCl	+0.07 (−0.05[b])	+0.18 (+0.27[b])
1 M KBr	+0.03 (−0.08[b])	+0.20 (+0.33[b])
1 M KSCN	+0.08 (−0.09[b])	+0.18 (+0.27[b])
1 M NaAc	+0.05 (−0.05[b])	+0.25 (+0.39[b])
1 M $CdAc_2$	+0.03 (−0.01[b])	+0.4 (+0.11[b])
1 M PbAc	+0.02 (−0.03[b])	+0.05 (+0.18[b])
1 M $CaCl_2$	−0.02 (−0.07[b])	+0.05 (+0.15[b])
1 M LiAc	−0.05	−0.02[b]

	MTCNQ/C Electrode[d]	
supporting electrolyte	initial scan oxidns[c]	redns on scan reversal[c]
1 M NaAc	+0.26	+0.12 (+0.02[b])
1 M KAc	+0.24	+0.12 (+0.01[b])

[a] Electrodes were prepared by mixing the neutral/metal salt with carbon (1:1 ratio) (graphite powder grade no. 38, Fisher Scientific, Fair Lawn, N.J.). [b] Peak potential. [c] Potential of onset of faradaic current; ([b]) indicates location of peak for this process, when observed. [d] NaTCNQ/C electrodes were used in 1 M NaAc and KTCNQ/C electrodes in 1 M KAc.

this electrode material, this possibility was investigated by irradiating the electrode surface during cyclic voltammetric scans with polychromatic xenon lamp light passed through either a distilled water or $CuSO_4$ solution filter and chopped at 1 Hz with a mechanical chopper. In the dark a 1 M potassium acetate solution containing 20 mM $K_4Fe(CN)_6$ showed a reversible cyclic voltammogram (e.g., Figure 3). When chopped light passed through a water filter irradiated the electrode, an increase in current was observed during the period of illumination. The magnitude and sign of the light effect were proportional to the magnitude and sign of the dark current as well as to the light intensity. When the dark current was anodic and large, the effect of the light was also large and in an anodic direction. In addition, the cyclic voltammetric waves did not exhibit the $t^{1/2}$ decay following the peak when the electrode surface was illuminated, but showed a positive deviation. When the light was filtered through a $CuSO_4$ solution, eliminating all but the visible radiation, the effect of the light was negligible. The band gap of TTF-TCNQ is around 0.1 eV[19] and thus it is not surprising that little response is observed from light in the visible region. The observed effect is probably attributable to heating at the electrode surface upon absorption of light by black TTF-TCNQ, causing convective stirring.

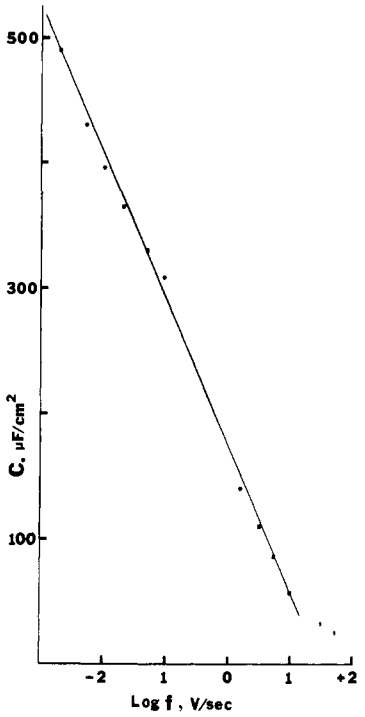

Figure 12. Apparent electrode double layer capacity (C_{dl}), $\mu F/cm^2$, for a TTF-TCNQ disk electrode in 1 M KCl as function of measurement frequency and scan rate. Low-frequency points determined by triangular scans between +0.124 and +0.073 V vs. SCE (electrode area, 0.49 cm^2). High-frequency points determined with ac bridge measurement at +0.190 V vs. SCE (electrode area, 0.096 cm^2).

Table IV. Redox Potentials for TTF and TCNQ Couples

redox couple	E, V vs. SCE	soln	electrode	ref
$TCNQ^0/TCNQ^-$	+0.115[a]	water/0.1 M $LiClO_4$	Pt	10
$TCNQ^-/TCNQ^{2-}$	−0.133[a]	water/0.1 M $LiClO_4$	Pt	10
$TCNQ^0/TCNQ^-$	+0.127[b]	CH_3CN/0.1 M $LiClO_4$	DME	9
$TCNQ^-/TCNQ^{2-}$	−0.291[b]	CH_3CN/0.1 M $LiClO_4$	DME	9
TTF^+/TTF^0	+0.30[a]	CH_3CH/0.1 M TEAP	(Pt?)	8
TTF^{2+}/TTF^+	+0.66[a]	CH_3CN/0.1 M TEAP	(Pt?)	8
TTF^+/TTF^0	+0.33[a]	CH_3CH/0.1 M TEAP	Pt	25
TTF^{2+}/TTF^+	+0.70[a]	CH_3CH/0.1 M TEAP	Pt	25

[a] Standard potentials, E^0. [b] Half-wave potential, $E_{1/2}$.

Discussion

The relative redox potentials of the TTF^+/TTF and $TCNQ/TCNQ^-$ couples in acetonitrile (Table IV), where all forms are soluble, indicate that electron transfer between TTF and TCNQ would not occur spontaneously if complex formation and precipitation did not occur.

$$TTF^+ + e = TTF^0 \quad E^0 = 0.32\ (\pm 0.02)\ \text{V vs. SCE} \quad (15)$$

$$TCNQ^0 + e = TCNQ^- \quad E^0 = 0.12\ (\pm 0.01)\ \text{V vs. SCE} \quad (16)$$

Wheland calculated an equilibrium constant for electron transfer of $10^{-2.2}$,[3] while optical measurements yield $10^{-2.6}$ [17] However, the formation of the TTF-TCNQ complex causes immediate reaction of TTF and TCNQ upon mixing in acetonitrile. Metzger[18] reported that the heat of the reaction

$$TTF(c) + TCNQ(c) \rightleftarrows TTF\text{-}TCNQ(c) \quad (17)$$

was $\Delta H^\circ = 37.41$ kJ/mol (0.388 eV/molecule). The added stabilization upon formation of the insoluble complex results in TTF being more difficult to oxidize and TCNQ being more difficult to reduce than the uncomplexed molecules. A rough estimate of the potentials for reduction and oxidation of TTF-TCNQ can be made by assuming that the entropy change in the reaction in eq 17 is negligible, so that $\Delta G^\circ \simeq \Delta H^\circ$, and that the energies of solvation in acetonitrile and water are nearly the same. Thus, from (15) and (16) we obtain

$$TTF^+ + TCNQ^0 + e = TTF\text{-}TCNQ(c)$$
$$E^\circ \simeq +0.71\ \text{V vs. SCE} \quad (18)$$

$$TTF\text{-}TCNQ(c) + e = TTF^0 + TCNQ^-$$
$$E^\circ \simeq -0.27\ \text{V vs. SCE} \quad (19)$$

These values are quite close to those found for the oxidation and reduction of the TTF-TCNQ lattice in LiAc (Table II and Figure 1). Note that the potentials for the TTF^{2+}/TTF^+ and $TCNQ^-/TCNQ^{2-}$ couples (Table IV) are such that continued oxidation to dication (at the positive limit) and reduction to the dianion (at the negative limit) are expected, consistent with the coulometric results in Table I and eq 1 and 3. The degree of charge transfer between TTF and TCNQ in the compound has been a subject of some interest and is currently taken as 0.59 ± 0.03,[20] so that this compound is sometimes written[18] $TTF^{+\rho}TCNQ^{-\rho}$ ($\rho = 0.59$). We should note that the electrochemical measurements reported here do not provide information about ρ, since they apply to overall reactions.

The assignment of the peaks which appear on reversal following the lattice oxidation and reduction processes was based on the coulometric results, a consideration of the chemical reactions which were possible in the different supporting electrolytes, a correspondence between the potentials at which these peaks occur and those found with the TTF/C and TCNQ/C electrodes, and the color of the electrode surface. The correspondence between the TTF/C and the TTF-TCNQ peaks with electrolyte anion (for TTF^+X^- reduction) and between the TCNQ/C and the TTF-TCNQ peaks with electrolyte cation (for M^+TCNQ^- oxidation) is shown in Figure 13. Unequivocal evidence for the formation of $TCNQ^0$ upon oxidation of TTF-TCNQ (eq 1) was obtained by in situ Raman spectroscopy of the electrode surface.[21] Correspondence between the disappearance of the TCNQ Raman signal and the voltammetric reduction peak is consistent with eq 2.

A more detailed and more quantitative interpretation of the observed redox processes at the TTF-TCNQ must await further studies. For example, $TCNQ^-$ is known to form dimers both in the solid state and in solution.[22] Reduction of TCNQ anion in aqueous media may also result in the formation of *p*-phenylenedimalonitrile ($TCNQH_2$).[23]

$$TCNQ^0 + 2e^- + 2H^+ \rightleftarrows TCNQH_2 \quad (20)$$

We have assumed in our explanations that these reactions were not of importance here. The location of the peaks suggests that TCNQ does not interact with other potential electron donors (e.g., halide ions) in solution. This is consistent with polarographic studies of TCNQ.[24] The integrated peak areas (Table I) depended upon the extent of lattice oxidation and reduction and corresponded to quantities of electricity of 20 to over 100 mC/cm^2 projected area (as opposed to 40 $\mu C/cm^2$ for a monolayer process). While this might be attributed to some porosity of the sintered electrode material and surface roughness, it appears that the oxidation or reduction of the lattice and the formation of the insoluble species (e.g., TTF^+Cl^- or

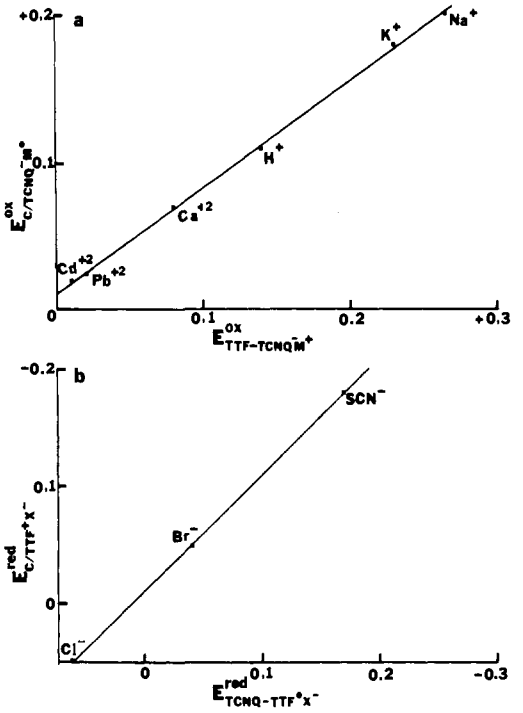

Figure 13. Correlation between measured potentials at TTF-TCNQ and TTF/C or TCNQ/C electrodes: (a) $TCNQ/M^+TCNQ^-$ couple potentials; (b) TTF^+X^-/TTF couple potentials. Supporting electrolyte concentration in all solutions was 1 M.

K^+TCNQ^-) occur over a multilayer thickness. Experiments are in progress with small electrodes made from single crystals of TTF-TCNQ to define more exactly the depth of electrochemical oxidation or reduction of the lattice. Experiments are also being conducted on other organic metallic-like compounds. Preliminary experiments show a similar potential region of stability for the TTT-TCNQ (TTT = tetrathiotetracene) complex. However, the NMP-TCNQ (NMP = *N*-methylphenazine) complex lattice is oxidized at less positive potentials.

The electrochemical behavior of these organic metallic-like compounds is of interest in connection with their practical use as electrodes in electroanalytical methods and for electrochemical devices, potentially replacing inert metal or carbon. The electrolysis of solution species may also be of use in the fabrication of devices from TTF-TCNQ, for example, in the deposition of copper or other metal to provide electrical contacts. Modification of the material surface by lattice oxidation or reduction and by substitution of electrolyte ions into the lattice may also be of interest.

Acknowledgment. The support of this research by the National Science Foundation and the Robert A. Welch Foundation is gratefully acknowledged. We are indebted to Dr. William Wallace for his many valuable suggestions and Raman spectroscopic analysis of the electrode surface. We also appreciate the helpful discussions with Dr. F. Wudl concerning this research.

References and Notes

(1) E. Engler, *Chemtech*, 274 (1976).
(2) J. Perlstein, *Angew. Chem., Int. Ed. Engl.*, **16**, 519 (1977).
(3) R. Wheland, *J. Am. Chem. Soc.*, **98**, 3926 (1976).
(4) E. Engler, B. Scott, S. Etemad, T. Penny, and V. Patel, *J. Am. Chem. Soc.*, **99**, 5909 (1977).
(5) P. Nielsen, A. Epstein, and D. Sandman, *Solid State Commun.*, **15**, 53 (1974).
(6) J. Torrance and B. Silverman, *Phys. Rev. B*, **15**, 788 (1977).
(7) R. Metzger, *J. Chem. Phys.*, **63**, 5090 (1975).
(8) R. Wheland and J. Gibson, *J. Am. Chem. Soc.*, **98**, 3916 (1976).
(9) L. Melby, R. Harder, W. Hertler, R. Benson, and W. Mochel, *J. Am. Chem. Soc.*, **84**, 3374 (1962).
(10) M. Sharp, *Anal. Chim. Acta*, **85**, 17 (1976).
(11) F. Kaufman, E. Engler, and D. Green, *J. Am. Chem. Soc.*, **98**, 1596 (1976).
(12) J. Chambers, D. Green, F. Kaufman, E. Engler, B. Scott, and R. Schumaker, *Anal. Chem.*, **49**, 802 (1977).
(13) R. J. Nowak, H. B. Mark, A. G. MacDiarmid, and D. Weber, *J. Chem. Soc., Chem. Commun.*, 9 (1977); R. J. Nowak, W. Kutner, and H. B. Mark, *J. Electrochem. Soc.*, **125**, 232 (1978).
(14) L. Melby, H. Harzler, and W. Sheppard, *J. Org. Chem.*, **39**, 2456 (1974).
(15) From the cell constants for TTF-TCNQ (T. Kistenmacher, T. Phillips, and D. Cowan, *Acta Crystallogr., Sect. B*, **30**, 763 (1974)), the maximum and minimum number of molecules of TTF and TCNQ at the surface of a 1-cm^2 electrode were calculated. It was assumed that there was equal probability that the electrode surface would consist of one of three different orientations with two molecules per unit cell. For both TTF and TCNQ there should be between 8.8×10^{13} and 2.8×10^{14} molecules/cm^2. If all surface species were oxidized or reduced this would produce approximately 8.5×10^{-5} C. Actual experiments, however, show approximately 9.6×10^{-3} C being consumed.
(16) R. N. Adams in "Electrochemistry of Solid Electrodes", Marcel Dekker, New York, 1969, p 219.
(17) Y. Tomkiewicz, J. Torrance, B. Scott, and D. Green, *J. Chem. Phys.*, **60**, 5111 (1974).
(18) R. Metzger, *J. Chem. Phys.*, **66**, 2525 (1977).
(19) A. Berlinsky, J. Carolan, and L. Weiler, *Solid State Commun.*, **15**, 795 (1974); U. Bernstein, P. Charkin, and P. Pincus, *Phys. Rev. Lett.*, **34**, 271 (1975); T. Pochler, A. Bloch, J. Ferraris, and D. Cowan, *Solid State Commun.*, **15**, 337 (1974).
(20) J. Fletcher and G. Toombs, *Solid State Commun.*, **22**, 555 (1977).
(21) W. Wallace, C. D. Jaeger, and A. J. Bard, submitted for publication. Raman spectra were recorded using a Cary 82 Raman spectrometer with the 4658-Å line of a Spectra Physics Model 164 Ar ion laser as the excitation source. The spectrum obtained corresponded in peak energies and relative peak intensities to previously published spectra of TCNQ.
(22) R. Boyd and W. Phillips, *J. Chem. Phys.*, **43**, 2927 (1965); M. Blandamer, K. Brwati, M. Fox, M. Symons, and G. Verma, *Trans. Faraday Soc.*, **63**, 1850 (1967).
(23) D. Acker and W. Hertler, *J. Am. Chem. Soc.*, **84**, 3370 (1962).
(24) M. Peover, *Trans. Faraday Soc.*, **60**, 417 (1964); R. Holm, W. Carper, and J. Blancher, *J. Phys. Chem.*, **71**, 3960 (1967).
(25) D. L. Coffen, J. Q. Chambers, D. R. Williams, D. E. Garraett, and N. D. Canfield, *J. Am. Chem. Soc.*, **93**, 2258 (1971).